Hue University Journal of Science: Natural Science
Vol. 131, No. 1D, 37–48, 2022

pISSN 1859-1388
eISSN 2615-9678

Optical properties of As_2S_3-based suspended-core photonic crystal fiber

Duc Hoang Trong[1], Nam Tran Hai[2], Thuy Nguyen Thi[1*]

[1] University of Education, Hue University, 34 Le Loi St., Hue, Vietnam
[2] Pham Van Dong High School, Ia Grai District, Gia Lai, Vietnam

* Correspondence to Thuy Nguyen Thi <nthuy@hueuni.edu.vn>
(*Received: 15 March 2022; Accepted: 19 April 2022*)

Abstract. In this paper, the nonlinear properties of photonic crystal fibers (PCF) with As_2S_3 substrate were analyzed numerically. With the suspended-core design, we achieve an anomalous dispersion regime with one or two zero-dispersion wavelengths, which is flat and has a small value at the investigated wavelength. The high nonlinear coefficient and very low confinement loss in the wavelength range of 1–3 μm, in comparison with other publications, are the outstanding advantages of these suspended-core PCFs. The highest nonlinear coefficient (28,527.374 $W^{-1}\cdot km^{-1}$), smallest effective mode area (0.593 μm^2), and low confinement loss (6.050×10^{-17} $dB\cdot m^{-1}$) at the wavelength of 1.55 μm were observed in the PCFs with a fiber diameter of 16.07 μm. Based on the numerical simulation results, we proposed two optimal structures suitable for supercontinuum generation.

Keywords: suspended-core PCF, flat dispersion, high nonlinear coefficient, low loss, supercontinuum generation

1 Introduction

Photonic crystal fiber (PCF) is a special type of optical waveguide based on photonic crystals, published in the 90s of the last century, and it attracted the attention of different research groups [1]. In recent years, the excellent propagation properties of PCFs, including linear and nonlinear parameters, have been investigated and controlled as desired [2-4]. Photonic crystal fibers have numerous applications in science and engineering [5-9] because of their outstanding optical properties. The PCF's design versatility via adjusting their lattice parameters to achieve exceptional optical properties, such as endlessly monomodal propagation, high nonlinearity, low confinement loss, and tunable chromatic dispersion profile, allow PCFs to be an excellent nonlinear medium to enhance supercontinuum (SC) generation performance [10-16]. In most studies on SC generation via PCFs, silica has been used as a common background material. However, the operating wavelength range is limited because of its high matter loss above the 2 μm wavelength, so it is difficult to generate SC in the infrared region. As a result, non-silica, such as chalcogenide glass, has great advantages in investigating nonlinear optical effects in PCFs because of the high nonlinearity of chalcogenide glasses in comparison with other glasses. This opens up the possibility of achieving interesting nonlinear properties in the longer wavelength range.

To improve the spectral range of SC light, researchers have already presented various designs, including selectively changing their cladding geometries, selecting a substrate material with a high nonlinear coefficient, or both to control the nonlinear properties of PCFs. In 2001, a new design of a microstructured optical fiber called “suspended-core fiber” was suggested

DOI: 10.26459/hueunijns.v131i1D.6723

by Monro et al. [17], with the preform geometry consisting of three holes centred on a central solid core. Then, Kiang et al. [18] reported a suspended-core fiber with lead-silicate glass in 2002. Kumar et al. and Petropoulos et al. [19, 20] also described a suspended-core fiber with tellurite and lead-silica glasses in 2003. Since then, suspended-core fiber has become a relatively new class of fibers and a subclass of microstructured fibers. The fiber microstructure consists of a triangular lattice of air holes that extend along the fiber. They surround a tiny central core with triangle geometry attached to a robust jacket with three thin struts [21].

The choice of high nonlinearity substrate material such as As_2S_3 is also an excellent solution to further improve the SC generation efficiency and achieve a broader, smoother, and better coherence SC spectrum. In 2013, Gao et al. [22] reported an As_2S_3 suspended-core fiber with a core diameter of 3.2 μm. Its nonlinear coefficient and the effective mode area at the 2.5-μm wavelength were 894.2 $W^{-1}{\cdot}km^{-1}$ and 8.43 μm^2. The SC generation process with a flat dispersion and zero-dispersion wavelengths (ZDWs) of 2.52 μm is investigated in detail. A chalcogenide (As_2S_3)-based ridge waveguide with a suspended structure on Si_3N_4 substrate was designed by Jing et al. [23] in 2018, which had low and flat dispersion profiles. Also, in 2018, the nonlinear coefficient and effective mode area of 561 $W^{-1}{\cdot}km^{-1}$ and 18.4 μm^2 at the 2-μm wavelength were achieved in an As_2S_3 suspended-core fiber with four holes fabricated by Si et al. [24]. Furthermore, the dispersion curve was relatively flat with a maximum of 14.19 $ps{\cdot}nm^{-1}{\cdot}km^{-1}$ at the 3-μmwavelength, and double zero-dispersion wavelengths in the infrared region were 2.59 and 3.63 μm.

Although these works achieved small and flat dispersions, they were beneficial for generating SC with a low nonlinear coefficient, a large effective mode area, and high loss. Simultaneous optimization of the optical properties of PCFs is an essential factor in improving SC generation efficiency, so many research groups have been focusing on this goal.

In this work, we selected an As_2S_3 composition glass, one of the types of chalcogenide glasses, as a promising material because of its high nonlinearity (100–500 times that of silica glass), low intrinsic loss of the material (0.01–0.1 $dB{\cdot}km^{-1}$), and potential to tailor dispersion [25]. The PCFs were designed with a suspended-core structure consisting of three air holes with various lattice parameters. Their optical properties were simulated and investigated in detail. The flat dispersion characteristics, high nonlinear coefficients, and very low confinement loss are the outstanding advantages of these PCFs.

2 Numerical modelling of PCFs

The Lumerical Mode Solutions software was used to design the structure and determine the modal properties of fibers. This software supports several higher-order modes apart from the fundamental mode. The arsenic trisulfide (As_2S_3) PCF used in this simulation has a suspended-core structure with three holes. Its cross-section geometrical structure is shown in Fig. 1a The light propagates in the defect of the fiber structure. To increase modal nonlinearity and optimize PCF structures, we designed PCFs with various lattice parameters, such as the radius of air holes, R_{hole}, the radius of the core, r_c (which was defined as the radius of the circle inscribed in the triangular core), the thickness of As_2S_3 bridge, t_c, and the diameter of the fiber, D. Fig. 1b shows that the light is strongly confined to the core of PCFs when R_{hole} = 7.615 μm; r_c = 0.41 μm; t_c = 0.125 μm, and D = 16.070 μm.

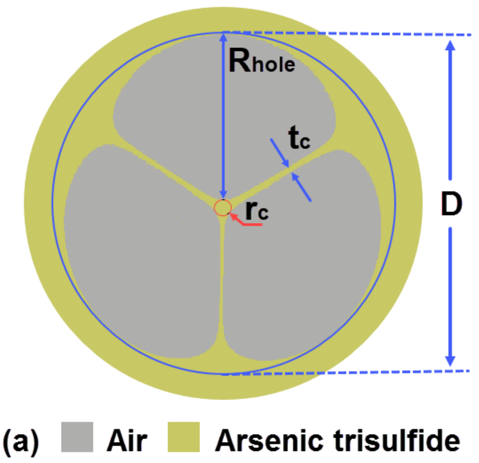

Fig. 1a. Cross-section geometrical structure of PCF with suspended core

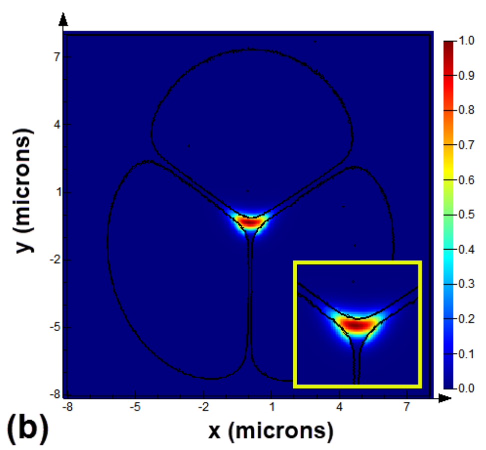

Fig. 1b. Light confined in core of PCF when $D = 16.07$ µm

With the As_2S_3 glasses, the refractive index as a function of wavelength is given in the four-term Sellmeier equation as [2]:

$$n^2 = 1 + \frac{1.9\lambda^2}{\lambda^2 - 0.022^2} + \frac{1.92\lambda^2}{\lambda^2 - 0.062^2} + \frac{0.87\lambda^2}{\lambda^2 - 0.122^2} \quad (1)$$

The numerical simulations were conducted for the PCFs with D changing from 16.07 to 64.28 µm by using the finite difference eigenmode (FDE) method. The process of FDE utilizes the Maxwell wave equation. The boundary condition is the perfectly matched layers to analyze the structure which makes no reflection at the boundary and reduces the loss. In addition, the fiber cross-section is divided into many rectangular sections to reduce meshing errors and increase the numerical accuracy of the simulations.

3 Optical properties of PCFs

3.1 Effective refraction index

The real part of the effective refractive indices corresponding to the fundamental mode over the wavelength range from 1 to 3 µm was found and shown in Fig. 2.

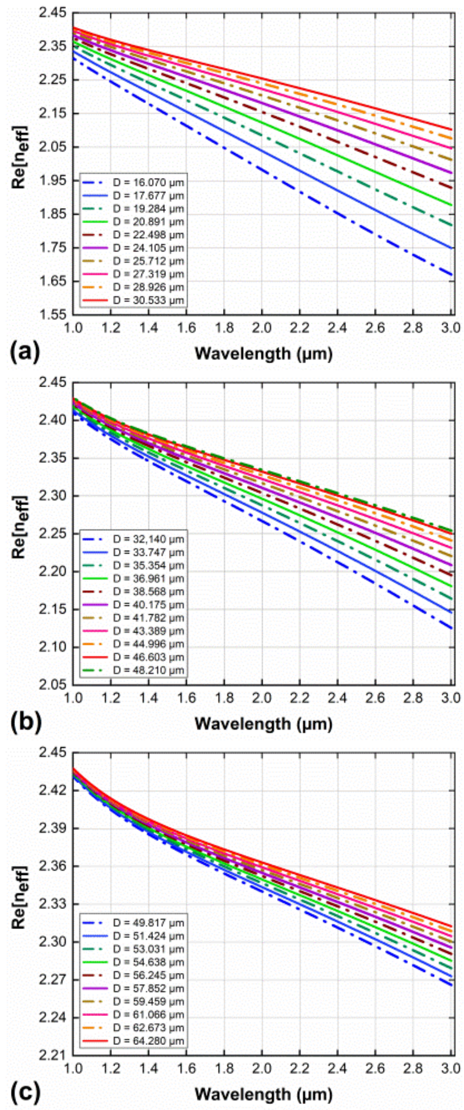

Fig. 2. Real part of effective refractive index as function of wavelength with various fiber diameters

For all cases, the real part of the effective refractive index (Re[n_{eff}]) decreases monotonically when the wavelength increases because of the stronger penetration of long wavelengths into the cladding region of PCFs. A change in the diameter of the fiber (D) strongly affects the Re[n_{eff}]; an increase in D causes the Re[n_{eff}] to increase. The refractive index of the medium's material varies when an intense input pulse propagates through the nonlinear medium, which causes the effective refraction index to change as well. The light interaction ability in the nonlinear medium of small-core PCFs is stronger than of the large-core PCFs, so the real part of the effective refraction index is larger in the case of a larger core.

The value of the real part of the effective refraction index of PCFs with various D is calculated at the 1.55 μm wavelength and displayed in Table 1. The maximum and minimum values of Re[n_{eff}] are 2.388 and 2.13 when D = 64.280 and 16.070 μm. The small difference between the two refractive index values for both cases is 0.258.

Table 1. Real part of effective refractive index at 1.55 μm wavelength of PCFs with various fiber diameters

D (μm)	Re [n_{eff}]	*D* (μm)	Re[n_{eff}]	*D* (μm)	Re[n_{eff}]
16.070	2.130	32,140	2.326	48.210	2.37
17.677	2.171	33.747	2.333	49.817	2.373
19.284	2.203	35.354	2.340	51.424	2.375
20.891	2.230	36.961	2.345	53.031	2.377
22.498	2.251	38.568	2.350	54.638	2.379
24.105	2.269	40.175	2.354	56.245	2.381
25.712	2.284	41.782	2.358	57.852	2.382
27.319	2.297	43.389	2.362	59.459	2.384
28.926	2.308	44.996	2.365	61.066	2.385
30.533	2.318	46.603	2.368	62.673	2.386
				64.280	2.388

3.2 Chromatic dispersion

We numerically calculated the chromatic dispersion coefficient of the PCFs, including both waveguide and materials dispersion by using the real part of the effective index according to the following formula

$$D_c = -\frac{\lambda}{c}\frac{d^2\,\mathrm{Re}\left[n_{\mathrm{eff}}\right]}{d\lambda^2} \tag{2}$$

where Re[n_{eff}] is the real part of n_{eff}, which is the effective index of a guided mode calculated by means the FDE method, and c is the velocity of light in the vacuum.

pISSN 1859-1388
eISSN 2615-9678

Fig. 3 illustrates the dispersion profiles of PCFs in terms of wavelength. As can be observed in this figure, the PCFs exhibit anomalous dispersion with a larger shift of zero-dispersion wavelengths towards the longer wavelength region as the fiber diameter increases. The large core fibers with a fiber diameter greater than 24.105 μm have anomalous dispersion with one ZDW. Meanwhile, anomalous dispersion with double ZDWs is observed in fibers with a smaller diameter. The zero-dispersion wavelength (ZDW1) is located around 1.45–1.65 μm, and the other (ZDW2) is from 1.83 to 2.84 μm. The two ZDWs divide the entire spectrum into three dispersion regions, i.e., a region with abnormal dispersion sandwiched between two regions with normal dispersion. Compared with a PCF with one ZDW, the soliton self-frequency shift has a clear redshift boundary that is close to the second ZDW [26]. The presence of a negative dispersion slope near the second ZDW causes a redshift in dispersive waves [27] in the second normal dispersion region and the trapped wave [28] because of phase matching between the redshifted soliton and the redshifted dispersive waves. The former effect broadens the supercontinuum to the red end, while the latter flattens the supercontinuum lying between redshift soliton and redshifted dispersive waves. For instance, an enhanced SC bandwidth with improved flatness was demonstrated in PCFs by generating two dispersive waves in the short- and long-wavelength sides of the SC spectrum [29]. Obviously, by carefully selecting the geometry of the structure and changing the lattice parameters in the simulation, we achieved anomalous dispersion with double ZDWs, similar to that of Si et al. [24], but it was not observed in other works [22, 23]. The anomalous dispersion with two ZDWs is one of the outstanding advantages of this work, suitable for some SC generations with the influence of soliton-induced effects.

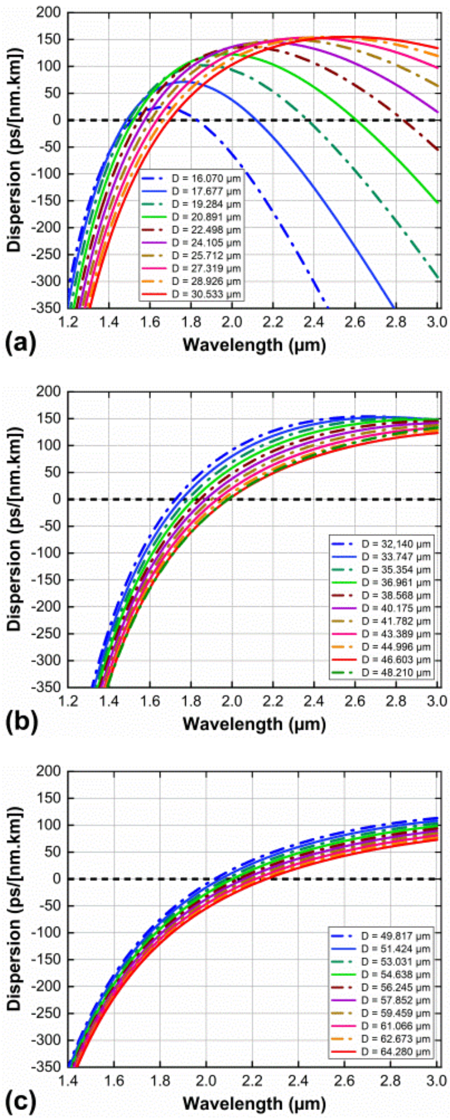

Fig. 3. Chromatic dispersion of PCFs with various fiber diameter

3.3 Effective nonlinearity

The nonlinear coefficient is one of the parameters that govern the SC spectral width because of the interaction of the input pulse with the nonlinear optical medium. To extend the SC spectrum further, we need the nonlinear coefficient as high as possible. The nonlinear coefficient (γ) is a measure of the nonlinearity of the medium, and it can be estimated according to Formula 3 [30].

DOI: 10.26459/hueunijns.v131i1D.6723

$$\gamma(\lambda) = 2\pi \frac{n_2}{\lambda A_{\mathrm{eff}}} \qquad (3)$$

where A_{eff} is the effective mode area for the basic mode of the fiber and n_2 is the nonlinear refractive index of the optical material (4.21 × 10^{-18} $m^2 \cdot W^{-1}$ at 1.55 μm) for As_2S_3 [31]. The effective mode area for the fundamental mode can be calculated according to Formula 4 [30], where E is the transverse electric field over the cross-section of the PCF

$$A_{\mathrm{eff}} = \frac{\left(\int_{-\infty}^{\infty} \int_{-\infty}^{\infty} |E|^2 \, dxdy \right)^2}{\int_{-\infty}^{\infty} \int_{-\infty}^{\infty} |E|^4 \, dxdy} . \qquad (4)$$

Using a material with a high nonlinear refractive index, such as As_2S_3, or paying attention to structural designs of PCFs for a smaller effective mode area (A_{eff}), or by a combination of both ways, can increase the value of the nonlinear coefficient. The variation of the nonlinear coefficient and the effective mode area as functions of wavelength is presented in Figs. 4 and 5.

The nonlinear coefficient has a large value (tens of thousands of $W^{-1} \cdot km^{-1}$) at short wavelengths and decreases with increasing wavelength. The light is no longer confined strongly inside the core of PCFs in the long-wavelength range because the modes get leaked through the holes and in between them, increasing the effective mode area. A small effective area is often observed in small-core fibers due to the strongly confined light in the core. This causes the nonlinear coefficient to decrease as the fiber diameter increases in the studied wavelength region.

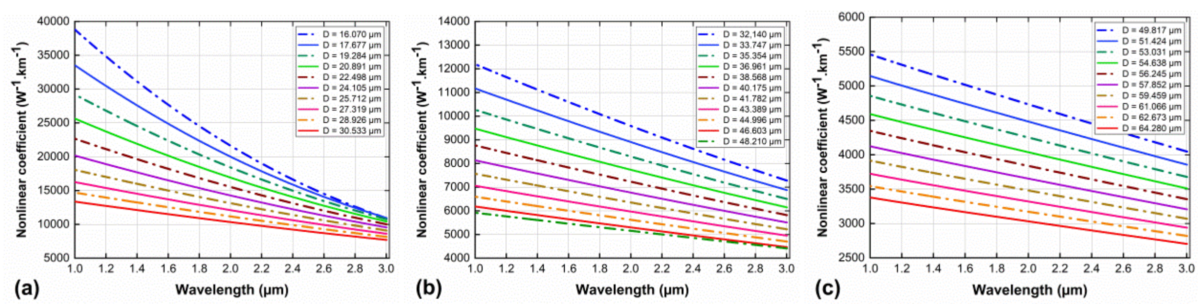

Fig. 4. Nonlinear coefficient of PCFs with various fiber diameter

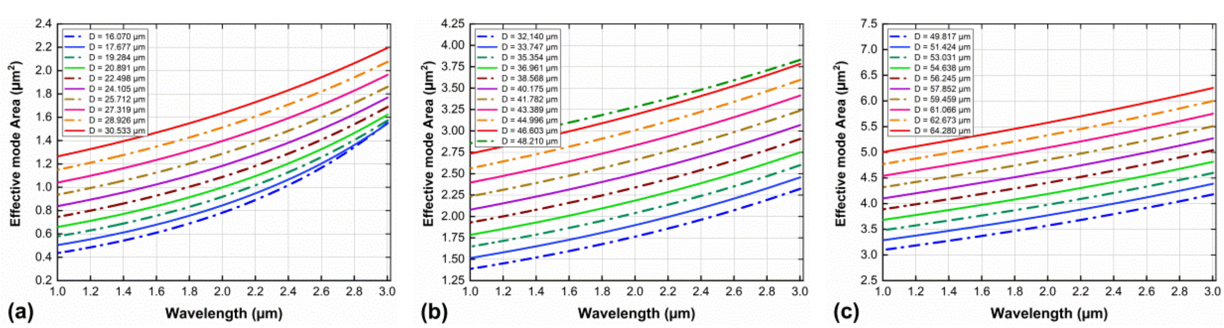

Fig. 5. Effective mode area of PCFs with various fiber diameter

pISSN 1859-1388
eISSN 2615-9678

The values of the nonlinear coefficients and the effective mode area at the 1.55 μm wavelength are presented in Tables 2 and 3. The maximum and minimum values of γ are 28,527.374 and 3,182.923 $W^{-1} \cdot km^{-1}$ when D is 16.07 and 64.28 μm. In contrast, the minimum and maximum values of A_{eff} are 0.593 and 5.312 μm^2 when D is 16.07 and 64.28 μm. We achieved much higher nonlinear coefficients and much smaller effective mode areas than those in other works [22, 24, 32, 33] with As_2S_3-based suspended-core PCFs.

The very high values of the nonlinear coefficients and very small values of the effective mode area are the outstanding advantages of this work. This is favourable for us to propose optimal PCF structures and study SC generation in future publications.

Table 2. Values of nonlinear coefficients at 1.55 μm wavelength of PCFs with various fiber diameters

D (μm)	**γ ($W^{-1} \cdot km^{-1}$)**	**D (μm)**	**γ ($W^{-1} \cdot km^{-1}$)**	**D (μm)**	**γ ($W^{-1} \cdot km^{-1}$)**
16.070	28527.374	32,140	10728.575	48.210	5496.674
17.677	25542.965	33.747	9900.805	49.817	5053.423
19.284	22902.698	35.354	9162.311	51.424	4774.345
20.891	20588.186	36.961	8501.258	53.031	4517.534
22.498	18566.324	38.568	7907.538	54.638	4280.721
24.105	16800.585	40.175	7372.577	56.245	4061.902
25.712	15256.294	41.782	6889.053	57.852	3859.321
27.319	13902.226	43.389	6450.766	59.459	3671.440
28.926	12711.121	44.996	6052.348	61.066	3496.862
30.533	11659.775	46.603	5689.220	62.673	3334.383
				64.280	3182.923

Table 3. Values of effective mode area at 1.55 μm wavelength of PCFs with various fiber diameters

D (μm)	**A_{eff} (μm^2)**	**D (μm)**	**A_{eff} (μm^2)**	**D (μm)**	**A_{eff} (μm^2)**
16.070	0.593	32,140	1.576	48.210	3.076
17.677	0.662	33.747	1.708	49.817	3.346
19.284	0.738	35.354	1.845	51.424	3.541
20.891	0.821	36.961	1.989	53.031	3.743
22.498	0.911	38.568	2.138	54.638	3.950
24.105	1.006	40.175	2.293	56.245	4.163
25.712	1.108	41.782	2.454	57.852	4.381
27.319	1.216	43.389	2.621	59.459	4.605
28.926	1.330	44.996	2.794	61.066	4.835
30.533	1.450	46.603	2.972	62.673	5.071
				64.280	5.312

3.4 Confinement loss

Confinement loss (L_c), an important parameter for generating SC spectra in PCFs, is determined from the PCF structural parameters, such as air-hole diameters, lattice types and constants, and the refractive index of the air-hole-filled material. It can be derived from the imaginary part of the effective refractive index of the PCF according to Formula 5 [33]

$$L_c = 8.686 \frac{2\pi}{\lambda} \mathrm{Im}[n_{\mathrm{eff}}(\lambda)]. \tag{5}$$

The confinement loss characteristics of the fundamental mode for the fibers are denoted in Fig. 6. It can be seen that the confinement loss decreases with the increase in fiber diameters. The confinement loss increases in the 2.6–3.0 μm wavelength region, which conforms to the change of absorption coefficients of As_2S_3 in the long-wavelength region. A very low value of confinement loss was achieved, approximately at 10^{-11} dB·m^{-1} for smaller fiber diameters. With the suspended-core structure of the designed PCFs, the modes are well confined in the core, and the electromagnetic field is primarily located there, resulting in a very low value of L_c. This is very beneficial for generating SC with a broadened spectrum. The very low values of L_c at the 1.55 μm wavelength can be found for fibers with larger diameters (Table 4). The highest value of L_c is 4.707 × 10^{-11} dB·m^{-1} with a fiber diameter of 16.07 μm. This L_c value is much lower than that of other publications [33], in which PCFs with selectively air-hole filled As_2S_5-As_2S_3 hybrid was designed by numerical modelling.

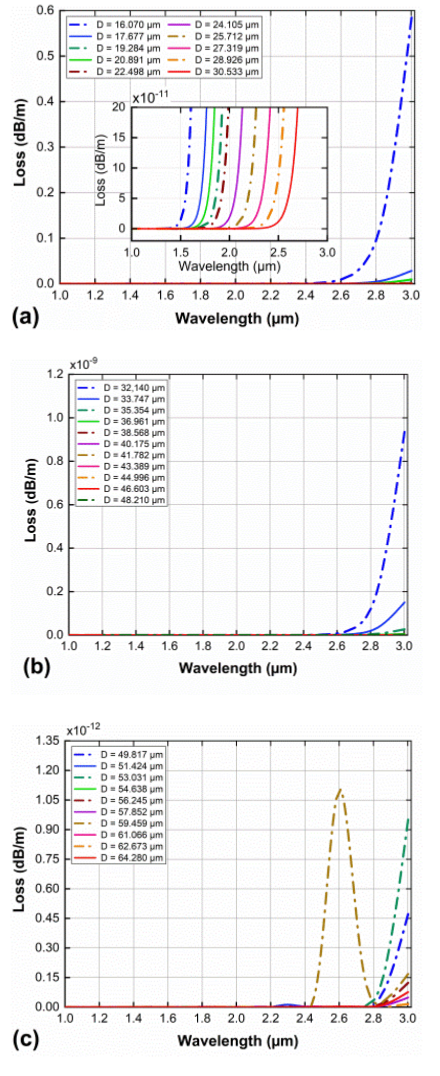

Fig. 6. Confinement loss of PCFs with various fiber diameters

Table 4. Values of confinement loss at 1.55 μm wavelength of PCFs with various fiber diameters

D (μm)	L_c (dB·m^{-1})	*D* (μm)	L_c (dB·m^{-1})	*D* (μm)	L_c (dB·m^{-1})
16.070	4.707×10^{-11}	32,140	-1.062×10^{-15}	48.210	6.050×10^{-17}
17.677	1.315×10^{-12}	33.747	-2.304×10^{-15}	49.817	-4.343×10^{-16}
19.284	5.424×10^{-14}	35.354	-6.000×10^{-17}	51.424	-1.466×10^{-16}
20.891	3.039×10^{-13}	36.961	-1.183×10^{-15}	53.031	1.314×10^{-16}
22.498	2.184×10^{-14}	38.568	1.260×10^{-16}	54.638	-4.913×10^{-16}

Hue University Journal of Science: Natural Science
Vol. 131, No. 1D, 37–48, 2022
pISSN 1859-1388
eISSN 2615-9678

D (μm)	L_c (dB·m⁻¹)	D (μm)	L_c (dB·m⁻¹)	D (μm)	L_c (dB·m⁻¹)
24.105	1.235×10^{-15}	40.175	6.290×10^{-16}	56.245	-3.855×10^{-17}
25.712	2.349×10^{-16}	41.782	-3.730×10^{-15}	57.852	-6.002×10^{-16}
27.319	-1.800×10^{-17}	43.389	7.670×10^{-16}	59.459	3.799×10^{-17}
28.926	-6.052×10^{-16}	44.996	1.554×10^{-15}	61.066	-1.446×10^{-18}
30.533	-2.081×10^{-16}	46.603	-7.035×10^{-16}	62.673	5.511×10^{-17}
				64.280	5.288×10^{-17}

3.5 Optimization of structural parameters of PCFs for SC generation

The optical pulse per unit distance of the propagation length of the fiber is changed by chromatic dispersion, so a PCF with suitable dispersion properties is a crucial condition dominating the efficiency of SC generation. The low anomalous dispersion near the ZDW, consisting of one ZDW and two ZDWs, provides the generation of a broad supercontinuum with strong confinement to the core despite low input power through soliton effects. Furthermore, the nonlinear properties, such as nonlinear coefficients, effective mode area, and confinement loss, contribute to generating new frequencies through the interaction of the input pulses with nonlinear media, such as PCFs. For that reason, two PCFs were proposed to consider for SC generation that must satisfy the above optical properties. Based on the above results, we introduce two structures, with D being 16.07 and 64.28 μm, which have flat anomalous dispersion, high nonlinear coefficients, and low confinement loss. Those two structures are named #F_1 and #F_2, with the lattice parameters shown in Table 5.

Fig. 7 shows the optical properties of the selected PCFs, where the optical properties of the #F_1 and #F_2 fibers are assigned blue and red. Both fibers exhibit anomalous dispersion properties. The #F_1 fiber with a smaller core diameter has two ZDWs, with a recommended pump wavelength of 1.55 μm, which is a practical common pumping wavelength of the laser, near the maximum value of dispersion. In contrast, the #F_2 fiber with a larger core diameter possesses flat anomalous dispersion, with one ZDW and has an expected pumping wavelength of 2.28 μm (Fig. 7a). In the studied wavelength region, the #F_2 fiber has a smaller dispersion value, but its effective mode area is larger than that of the #F_1 fiber because of its large core, which means that the #F_1 fiber gets a higher nonlinearity coefficient. The confinement loss of the #F_1 fiber is also higher than that of the #F_2 fiber (Figs. 7b and 7c). Note that we have a priority to control how the structure is designed to suit the application purpose since the optical properties of PCFs are difficult to optimize simultaneously. In this paper, both selected PCFs are suitable for SC generation because of their advantages according to each separate optical property. The nonlinear characteristic values at the pump wavelength are introduced in Table 6 in comparison with those of some previous publications on As_2S_3-based PCFs.

Table 5. Lattice parameters of two proposed PCFs

#	D (μm)	R_{hole} (μm)	r_c (μm)	t_c (μm)
#F_1	16.07	7.615	0.41	0.125
#F_2	64.28	30.46	1.64	0.5

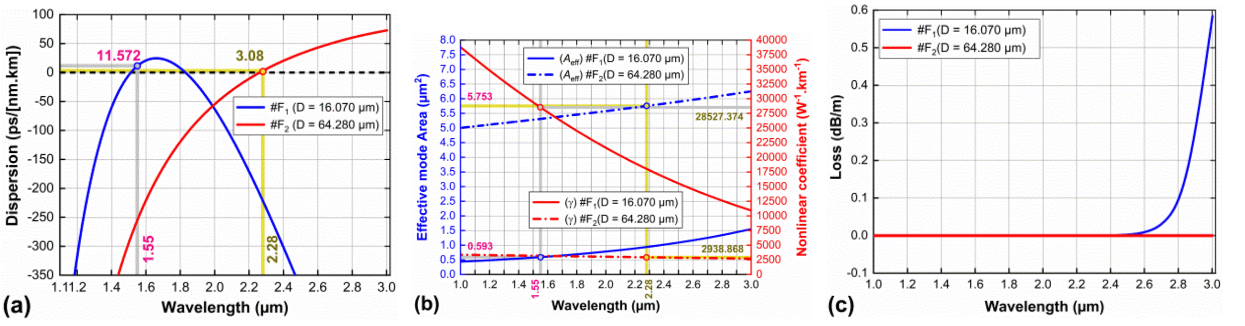

Fig. 7. Optical properties of the proposed PCFs with various fiber diameter (a) chromatic dispersion, (b) nonlinear coefficient and effective mode area, and (c) confinement loss

Table 6. Comparison of nonlinear characteristic values at pump wavelength of proposed PCFs with some previous publications on As_2S_3-based PCFs

#	Refs., Year	D (μm)	Pump wavelength (μm)	D_c (ps·nm·km⁻¹))	γ (W^{-1}·km^{-1})	A_{eff} (μm²)	L_c (dB·m⁻¹)
#F_1 (this work)		16.070	1.55	11.572	28527.374	0.593	4.707×10^{-11}
#F_2 (this work)		64.280	2.28	3.08	2938.868	5.753	4.615×10^{-16}
PCF with suspended core As_2S_3	Weiqing, 2013	160	2.5	–	894.2	8.43	1.0
PCF with suspended core As_2S_3	Nian, 2018	5.0	2.0	14.19	561	18.4	5.7
Suspended core As_2S_3 tapered fiber	Imtiaz, 2020	11.5	1.938	−8.32	3210	–	–
As_2S_5-As_2S_3 hybrid PCF	Chen, 2017	–	4.5	0.025	104	25.7	3.7×10^{-7}

4 Conclusion

In this paper, we reported on the optical properties of As_2S_3-based suspended-core photonic crystal fibers with changing lattice parameters. The anomalous dispersion with two zero-dispersion wavelengths, a very high nonlinear coefficient, a small effective mode area, and a low confinement loss in comparison with previous works are the highlights of our work. Two structures with optimal properties were proposed and analyzed in detail to show their outstanding advantages in SC generation orientation.

Funding statement

This research is funded by the Vietnam National Foundation for Science and Technology Development (NAFOSTED) and Vietnam's Ministry of Education and Training under grant numbers 103.03-2020.03 and B2021- DHH-08.

pISSN 1859-1388
eISSN 2615-9678

References

1. Dudley JM, Genty G, Coen S. Supercontinuum generation in photonic crystal fiber. Review of Modern Physics. 2006;78(4):1135.
2. Mona Kalantari, Arash Karimkhani, and Hamed Saghaei. Ultra-Wide mid-IR supercontinuum generation in As_2S_3 photonic crystal fiber by rods filling technique. Optik. 2018;158: 142-10. DOI: https://doi.org/10.1016/j.ijleo.2017.12.014.
3. Ghanbari A, Kashaninia A, Sadr A, Saghaei H. Supercontinuum generation for optical coherence tomography using magnesium fluoride photonic crystal fiber. Optik. 2017;140:545-10.
4. Saghaei H, Heidari V, Ebnali-Heidari M, Yazdani MR. A systematic study of linear and nonlinear properties of photonic crystal fibers. Optik - International Journal Light and Electron Optics. 2016;127(24):11938-10.
5. Sanchez-Cano A, Saldana-Diaz JE, Perdices L, Pinilla I, Salgado-Remacha FJ, Jarabo S. Measurement method of optical properties of ex vivo biological tissues of rats in the near-infrared range. Applied Optics. 2020;59(13):D111-7.
6. Jiang Z, Wang T, Sun Z, Lin P, Yu C, Ma W. Transmission of low-noise supercontinuum based wide-spectral carriers in a simulated atmosphere channel with tunable turbulence. Optics Communications. 2020;458:124830.
7. Halloran M, Traina N, Choi J, Lee T, and Yoo J. Simultaneous measurements of light hydrocarbons using supercontinuum laser absorption spectroscopy. Energy Fuels. 2020;34(3):3671-8.
8. Lu R, Beers RV, Saeys W, Li C, Cen H. Measurement of optical properties of fruits and vegetables: a review. Postharvest Biology Technology. 2020;159:111003.
9. Jiang Y, Karpf S, Jalali B. Time-stretch LiDAR as a spectrally scanned time-of-flight ranging camera. Nature Photonics. 2020;14:14-5.
10. Agrawal GP. Nonlinear Fiber Optics (6th ed.). London: Academic press; 2019.
11. Rutkauskas M, Srivastava A, Reid DT. Supercontinuum generation in orientation-patterned gallium phosphide. Optica. 2020;7:172-4.
12. Lanh VC, Hoang VT, Long VC, Borzycki K, Xuan KD, Quoc VT, et al. Optimization of optical properties of photonic crystal fibers infiltrated with chloroform for supercontinuum generation. Laser Physics. 2019;29(7):075107.
13. Van LC, Hoang VT, Long VC, Borzycki K, Xuan KD, Quoc VT, et al. Supercontinuum generation in photonic crystal fibers infiltrated with nitrobenzene. Laser Physics. 2020;30(3):035105.
14. Chu Van L, Nguyen Thi T, Le Tran BT, Trong DH, Thi Minh NV, Van Le H, et al. Multi-octave supercontinuum generation in As_2Se_3 chalcogenide photonic crystal fiber. Photonics and Nanostructures - Fundamentals and Applications. 2022;48:100986.
15. Thi TN, Trong DH, Le Tran BT, Van TD, Van LC. Optimization of optical properties of toluene-core photonic crystal fibers with circle lattice for supercontinuum generation. Journal of Optics. 2022;51(3):678-88.
16. Abdelkader Medjouri, Djamel Abed. Theoretical study of coherent supercontinuum generation in chalcohalide glass photonic crystal fiber. Optik. 2020;219:165178.
17. Tanya MM, Walter B, Kentaro F, Joanne CB, Broderick NGR, Richardson DJ. Sensing with microstructured optical fibres. Measurement Science and Technology. 2001;12(7):854.
18. Kiang KM, Frampton K, Monro TM, Moore R, Tucknott J, Hewak DW, et al. Extruded singlemode non-silica glass holey optical fibres. Electronics Letters. 2002;38(12):546-7.
19. Kumar VVRK, George AK, Knight JC, Russell PSJ. Tellurite photonic crystal fiber. Opt Express. 2003;11(20):2641-5.
20. Petropoulos P, Ebendorff-Heidepriem H, Finazzi V, Moore RC, Frampton K, Richardson DJ, et al. Highly nonlinear and anomalously dispersive lead silicate glass holey fibers. Opt Express. 2003;11(26):3568-73.
21. Mouawad O, Picot-Clémente J, Amrani F, Strutynski C, Fatome J, Kibler B, et al. Multioctave midinfrared supercontinuum generation in suspended-core chalcogenide fibers. Opt Lett. 2014;39(9):2684-7.
22. Gao W, El Amraoui M, Liao M, Kawashima H, Duan Z, Deng D, et al. Mid-infrared supercontinuum generation in a suspended-core As_2S_3 chalcogenide microstructured optical fiber. Opt Express. 2013;21(8):9573-83.
23. Jing S, Mei C, Wang K, Yuan J, Yan B, Sang X, et al. Broadband and highly coherent supercontinuum

generation in a suspended As_2S_3, ridge waveguide. Optics Communications. 2018;428:227-32.

24. Si N, Sun L, Zhao Z, Wang X, Zhu Q, Zhang P, et al. Supercontinuum generation and analysis in extruded suspended-core As_2S_3 chalcogenide fibers. Applied Physics A. 2018;124(2):171.

25. Xiong C, Magi E, Luan F, Tuniz A, Dekker S, Sanghera JS, et al. Characterization of picosecond pulse nonlinear propagation in chalcogenide As_2S_3 fiber. Appl Opt. 2009;48(29):5467-74.

26. Skryabin DV, Luan F, Knight JC, Russell PStJ. Soliton self-frequency shift cancellation in photonic crystal fibers. Science. 2003;301(5640):1705-4.

27. Genty G, Lehtonen M, Ludvigsen H. Effect of cross-phase modulation on supercontinuum generated in microstructured fibers with sub-30 fs pulses. Opt Express. 2004;12(19):4614-24.

28. Wang W, Yang H, Tang P, Zhao C, Gao J. Soliton trapping of dispersive waves in photonic crystal fiber with two zero dispersive wavelengths. Opt Express. 2013;21(9):11215-26.

29. Mussot A, Beaugeois M, Bouazaoui M, Sylvestre T. Tailoring CW supercontinuum generation in microstructured fibers with two-zero dispersion wavelengths. Opt Express. 2007;15(18):11553-63.

30. Agrawal G. Agrawal G, editor. Nonlinear Fiber Optics (Fifth Edition). Boston: Academic Press; 2013.

31. Laniel JM, Hô N, Vallée R, Villeneuve A. Nonlinear-refractive-index measurement in As_2S_3 channel waveguides by asymmetric self-phase modulation. J Opt Soc Am B. 2005;22(2):437-45.

32. Alamgir I, Shamim MHM, Amraoui ME, Messaddeq Y, Rochette M, editors. Supercontinuum Generation in Suspended Core As_2S_3 Tapered Fiber. 2020 IEEE Photonics Conference (IPC); 2020 28 Sept.-1 Oct. 2020.

33. Wei C, Zhang H, Luo H, Shi H, Liu Y. Broadband mid-infrared supercontinuum generation using a novel selectively air-hole filled As_2S_5-As_2S_3 hybrid PCF. Optik. 2017;141:32-8.